Natural Hazards (2021) 107:1387–1411
https://doi.org/10.1007/s11069-021-04636-6

ORIGINAL PAPER

Study on stability of exit slope of Chenjiapo tunnel under extreme rainstorm conditions

Xiang Duan[1] · Tian-shun Hou[1] · Xiao-dong Jiang[1]

Received: 7 September 2020 / Accepted: 10 February 2021 / Published online: 4 March 2021

Abstract

The exit slope of the Chenjiapo tunnel is located in Xuanen County, Hubei Province, China, and rainfall is one of the main factors inducing landslides. During the tunnel excavation, the left side of the front edge of the slope slid downward and caused a 6.27×10^4 m^3-large landslide. Moreover, a 8.69×10^5 m^3-large unstable slope was formed under the combined action of rainfall and the excavation. Because the front edge of the slope has been sliding, further tunnel excavation and extreme rainfall may induce massive landslides. This not only threatens the safe construction of the tunnel but also directly risks the operation safety of the expressway at a subsequent stage. To reveal the failure process of the Chenjiapo tunnel exit slope under extreme rainfall conditions, the slope stability is studied under five rainfall types and three rainfall intensities by conducting numerical simulations using the GeoStudio software. The results show that under the condition of front-peak rainfall, the safety factor of the slope first decreases and subsequently increases with increasing rainfall time. The slope is damaged at the 18th hour of the rainfall, and the plastic zone completely penetrates the upper soil layer at the end of the first day of the rainfall. In addition, the maximum horizontal displacement of the slope, which is up to 0.233 m, is the maximum among those under the five rainfall types. Under the conditions of equal-intensity, stepped, medium-peak, and back-peak rainfall, the safety factor of the slope decreases with increasing rainfall time. The slope begins to be destroyed between the second and the third days of the rainfall, and the plastic zone begins to be fully penetrated. Therefore, for the same rainfall time and total rainfall amount, the front-peak rainfall is the most harmful to the slope stability. Under 50, 70, and 90 mm/day rainfall intensities, the safety factor of the slope decreases with increasing rainfall time. Compared with the other two rain intensities, the slope is damaged first at the 27th hour under the 90 mm/day-rain intensity. At the end of the rainfall, the safety factor of the slope is the smallest under the rainfall intensity of 90 mm/day, which is 0.887. This indicates that a high rainfall intensity is associated with easy damage to the slope. After the rainfall, the safety factor of the slope immediately recovers, the horizontal displacement gradually rebounds, the distribution range of the plastic zone begins to decrease, and the slope returns to a stable state after 12 days of the rainfall ending. The exit slope of the Chenjiapo tunnel may fail under extreme rainfall conditions; therefore, it is urgent to adopt reinforcement measures, such as an anti-slide pile as the main support and drainage and sealing slope cracks as the auxiliary ones.

Extended author information available on the last page of the article

Keywords Chenjiapo tunnel · Slope stability · Finite element method · Rainfall model · Safety factor

1 Introduction

Many factors affect slope stability, such as rainfall, earthquakes, reservoir impoundment, and weathering. Among them, rainfall is the most important factor inducing landslides (Yu et al. 2008; Shi et al. 2016; Huang et al. 2017). Based on statistics, landslides caused by rainfall account for approximately 70% of the total number of landslides, and 95% of these occur in the rainy season. These landslides cause serious casualties and large economic losses. Because of their high frequency, wide distribution, and complex damage, rainfall landslides are one of the main types of landslide disasters, which have the characteristics of large scale, rapid development, and massive destruction (Ye and Shi 2018). Therefore, examining the relationship between rainfall and landslides is the key to studying and preventing landslide geological disasters.

The influence of rainfall on slope stability has been studied by numerous scholars. By scripting and verifying the calculation program of slope stability under transient water pressure, it was found that rainfall infiltration forms a transient saturation zone on the surface of a slope (Jiang et al. 2015a, b). A thick transient saturation zone implies a small slope safety factor. After the transient saturation zone reaches a certain depth, the safety factor decreases to a minimum value and remains unchanged. By a comprehensive study of the causes of the Kasavu landslide instability and the mechanism of slope failure, it was found that 361 mm of rainfall in the early three days and 176 mm of average daily rainfall were its main trigger factors (Ram et al. 2019). Analysis of a bedding landslide at the construction site of the Sanli Expressway in Guizhou Province showed that it is mainly triggered by continuous rainfall, and the main objective factors affecting its occurrence are steep slopes (the maximum inclination angle is 46°), rock strata, bedding characteristics of the weak interlayers, and generation of free surfaces by slope excavation (Zhao et al. 2019). The causes of more than 600 shallow landslides in Mocoa were studied by analyzing the local topography, landslide data, rainfall data, and satellite images. It was found that early rainfall and heavy rainfall were the main trigger factors of these shallow landslides (Garcia-Delgado et al. 2019). By studying the Carpathian flysch landslide in Poland, it was found that the rise in the slope groundwater level was caused by rainstorms and rainwater infiltration, and the change in the pore water pressure was the key factor that accelerated the landslide (Bednarczyk 2018). In view of the influence of rainfall on slope failure, a two-phase material point method formula was proposed (Wang et al. 2018). The results showed that initially a slope is stable. Subsequently, rainfall affects the shear strength of the soil, and it decreases with the decreasing slope from the surface. Finally, the slope surface begins to damage and subsequently is completely destroyed.

A numerical analysis method can overcome the limitations of the traditional analysis method and analyze the nonlinear stress and strain of a slope of any shape. In a study, the typical landslide project of the Yuanmo Highway was selected, and the FLAC^{3D} finite difference method simulation software was used to analyze the stability of the actual slope engineering under the condition of heavy rainfall. It was found that under heavy rainfall, a large amount of rainwater infiltration increases the saturated area of the slope, and the stability of the slope decreases significantly (Rong et al. 2008). Using the GeoStudio finite element simulation software to simulate a homogeneous soil slope, it was found that the change in the water level and the seepage field in the slope caused by rainfall destroy the stability of the slope (Jiang et al. 2015a, b). The FLAC two-phase flow module was used to simulate the infiltration process of water and explore the influence of rainfall duration on the distribution of the most dangerous slip surface of a slope. It was found that a long rainfall duration is associated with a low probability of the most dangerous slip surface to be located in the bedrock of the slope bottom (Dou and Wang 2017). The limit equilibrium method was utilized, and finite element numerical simulations were conducted to analyze the slope stability of Wanjia Middle School in the Wenchuan earthquake area, respectively. The finite element method results were consistent with those of the limit equilibrium method, and they suggested that shallow landslides are probable to occur under the conditions of rainstorms or earthquakes (Hou et al. 2016). Finite element analysis of unsaturated soil mechanics was performed to comprehensively study the failure of a geosynthetic-reinforced soil slope under rainfall. It was found that the development of positive pore water pressure in the reinforced belt and the action of the retained weathered sandstone layer were the main factors inducing slope failure (Yang et al. 2019). A finite element coupling analysis of the failure and deformation mechanisms of two unstable unsaturated slopes was conducted (Yang et al. 2017). The numerical results showed that rainfall reduces the matrix suction of the slopes and the shear strength of the soil, which leads to the failure of the slopes.

Regarding multi-field coupling, a fluid–solid coupling finite element model of an unsaturated soil was established and the seepage field and stress field of a slope were comprehensively analyzed under rainfall conditions. It was found that a high rainfall intensity implies a large slope deformation, and a shallow slope is more prone to plastic failure (Xu et al. 2005). In another study, based on a multi-field coupling analysis of the seepage, stress, and displacement fields in a rainfall landslide, it was revealed that the slope stress and displacement fields change with the change in the slope seepage field during rainfall (Gao et al. 2014). Regarding early rainfall, it was found that the degree by which the slope stability is affected by the early rainfall is related to the permeability coefficient of the slope soil. Generally, a small permeability coefficient implies a strong influence of the early rainfall on the slope stability (Tang et al. 2013). By conducting numerical simulations of shallow-flow landslides, it was found that combined early and single rainfall event is the main factor causing slope failure (Santo et al. 2018). By studying the influence of different rainfall intensities on slope stability, it was found that a low-intensity early rainfall implies a large initial safety factor of the slope (Zeng et al. 2018). Regarding the delayed influence of rainfall, by analyzing the change process of slope stability after rainfall, it was found that the most unstable time of a slope occurs after the slope rainfall, and not during it (Kong et al. 2013). The failure process of an expansive soil slope induced by rainfall was studied. It was determined that rainfall can induce a gradual failure of the slope from the foot to the top of the slope, and the slope is not destroyed until the rainfall stops for a period. Specifically, slope failure has clear characteristics of rainfall lag (Zhang et al. 2019). Regarding the slope of an expansive soil, by studying the Houba landslide in the three Gorges Reservoir area, it was found that slope deformation mainly occurred in the surface layer of the expansive soil layer. Moreover, rainstorms and continuous rainfall are the main causes of the slope instability (Hou et al. 2013). To explore the reasons for the shallow failure of the expansive soil slope, numerical simulations of such slope were conducted under different rain intensities, rain times, and slope ratios. It was found that the slope safety factor decreases with the increase in the rain intensity and the rain time. Even under the condition of a very small slope ratio, the expansive soil slope remains unstable (Zhan et al. 2018).

Although a numerous scholars have analyzed the change process of slope stability under rainfall conditions and achieved useful achievements, few researchers have studied gravel slope. Generally, the upper soil permeability of such a slope is low, the infiltration rate of rainwater is slow under rainfall conditions, and the surface soil of the slope is first transformed into a saturation state. Subsequently, with the infiltration of rainwater, the saturation line rises and the internal soil gradually saturates. Because of its high gravel content, large pores, and relatively high permeability, the rainwater rapidly infiltrates under rainfall conditions, which can cause the soil internal saturation line to rise. Therefore, initially, the internal soil in a gravel slope is saturated, and subsequently as the saturation line further rises, the surface soil gradually saturates. The exit slope of the Chenjiapo tunnel is a typical gravel slope, and the slope of its sliding body mainly comprises collapsed and deposited gravel soil with a high gravel content, local block stone, and siltstone bedrock. At present, local landslides occur on the left side of the front edge of the slope. Under the condition of heavy rainfall or continuous rainfall, the entire slope may be unstable, which seriously threatens the safe construction of the tunnel and the performance safety of the expressway at a later stage.

Therefore, in this study, regarding the exit slope of the Chenjiapo tunnel, the GeoStudio finite element software is used for conducting the numerical simulation. By simulating the dynamic change process of the slope stability from natural to rainfall conditions, the mechanism of the slope instability caused by rainfall is explored. Moreover, the effects of different rainfall types and rain intensities on the dynamic change process of the slope stability are studied. Therefore, the research results can provide the basis for the protection and treatment of such slopes.

2 Engineering scenario of Chenjiapo tunnel exit slope

The exit slope of the Chenjiapo tunnel is located in Qinjiaping Village, Xiaoguan Township, Xuanen County, Enshi City, Hubei Province. During the excavation of the tunnel, the left side of the front edge slope slipped downward, and a sliding landslide body and an unstable slope body were formed under the action of rainfall and the excavation. The landslide body has an irregular fan shape on the plane, the main slip direction is 135°, the width is approximately 120 m, the longitudinal length is approximately 70 m, and the volume of the landslide body is approximately 6.27×10^4 m^3. The thickness of the upper loose overburden of the sliding landslide body is 8–30 m, and the left and right overburdens are relatively thinner and thicker, respectively. The back and front edge elevations of the slope are 756.0 and 722.0 m, respectively, and the relative height difference is approximately 34 m. The back and front edge elevations of the potential landslide area of the unstable slope are approximately 822.5 and 722.0 m, respectively, and the relative height difference is approximately 100 m. The average thickness of the sliding landslide body is approximately 20.8 m, its width is approximately 200 m, the longitudinal length is approximately 300 m, and the volume is approximately 8.69×10^5 m^3. The engineering geological map and longitudinal section of the slope are shown in Figs. 1, 2, respectively.

Qinjiaping Village is located in the middle latitudes, and it belongs to the subtropical monsoon climate region. It has the characteristics of high average temperature, humid air, abundant rainfall, distinct seasons, cold winter, and hot summer. It has an internal monsoon climate, the rainfall has regional zonation in the horizontal and vertical directions, and the rainfall is substantial during the rainstorm season. The heterogeneity of the rainfall amount

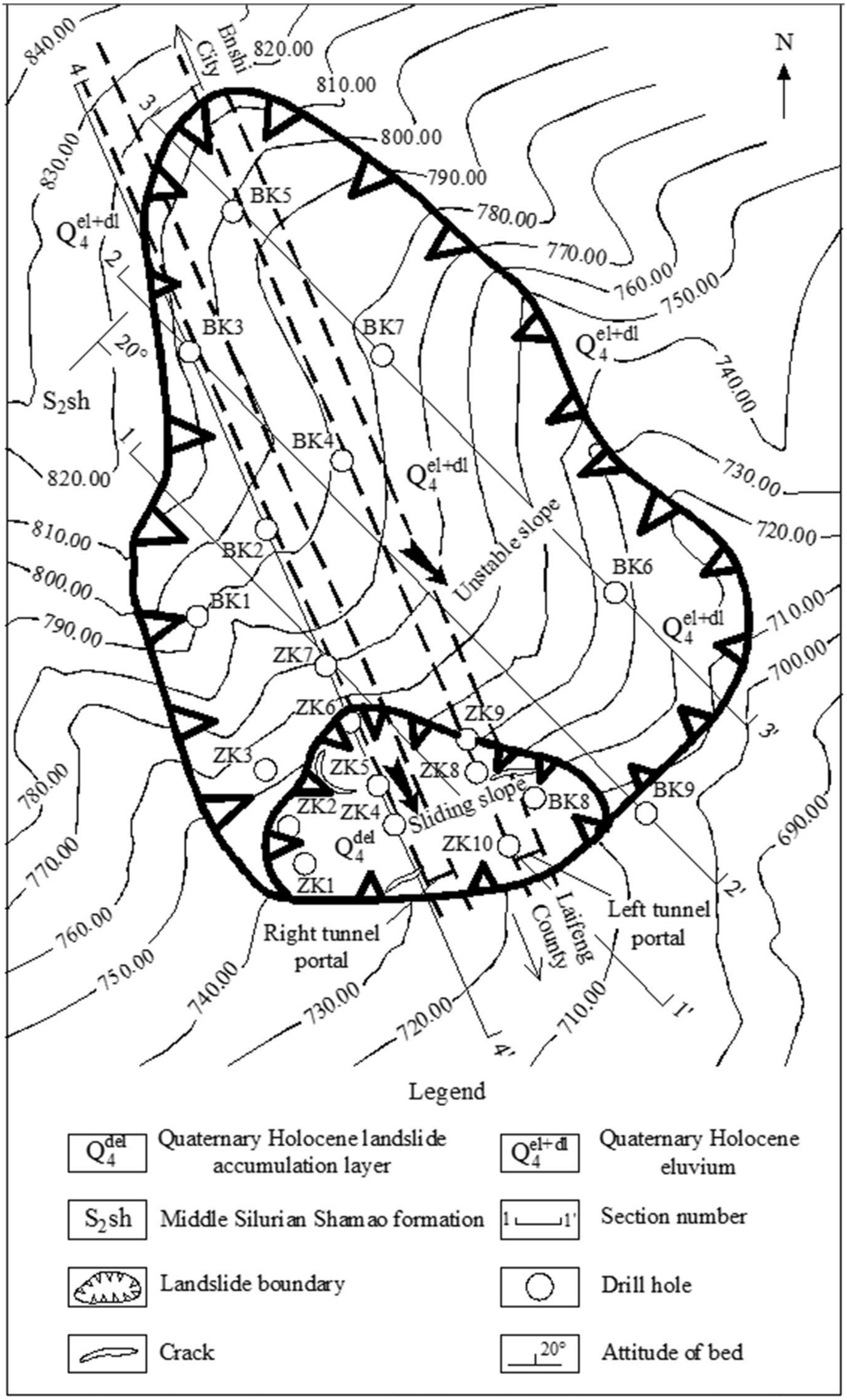

Fig. 1 Engineering geological map of slope

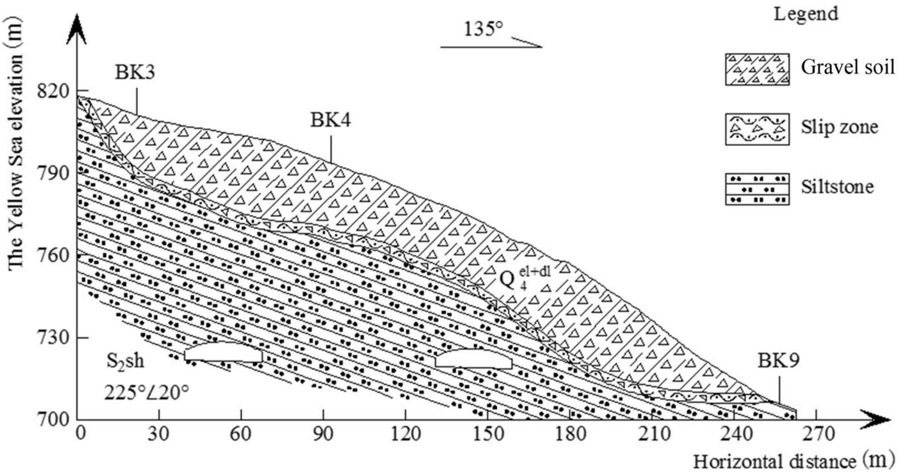

Fig. 2 Longitudinal section (2–2′) of slope

and the rainfall days in the time–spatial distribution as well as the characteristics of frequent rainstorms, continuous rainfall, high-intensity rainfall, and sudden rainfall in spring and summer are two of the main factors inducing landslides. The sliding landslide body threatens the safe construction of the tunnel, and the tunnel is in a state of shutdown. The unstable slope not only risks the safe construction of the tunnel but also directly threatens the operation safety of the expressway at a subsequent stage, which may cause a certain loss of life and property.

3 Computational model

GeoStudio is a set of professional, efficient, and powerful simulation analysis software for geotechnical engineering and geotechnical environment simulation calculation, which includes SEEP/W, SIGMA/W, and SLOPE/W modules. The SEEP/W module is a very important module in the GeoStudio software, which is a professional analysis software for unsaturated soil seepage. The SLOPE/W module is one of the most advanced geotechnical slope stability analysis software worldwide, and the finite element method can be used to calculate and analyze most slope stability problems effectively. The SIGMA/W module is a professional software for the stress and deformation analysis of geotechnical structures; it can solve linear elastic deformation problems and highly complex nonlinear elastoplastic problems.

3.1 Calculation principle and method

1. Darcy's law and finite element seepage equation.

Darcy's law of saturated and unsaturated soil seepage is expressed as follows:

$$q = ki$$

where q is the flow per unit volume, k is the permeability coefficient, and i is the total water head gradient. Darcy's law was originally derived based on saturated soil seepage;

however, subsequent research showed that it can also be applied to unsaturated soil seepage. The only differences between saturated and unsaturated soil seepage are that the permeability coefficient is not constant under unsaturated conditions and that the permeability coefficient changes directly and indirectly with changing water content and water pressure, respectively. By adopting Darcy's law of unsaturated soil seepage in the SEEP/W module, the finite element equation of seepage analysis is obtained, which simulates and calculates the seepage problems of unsaturated soil.

2. Morgenstern–Price method for slope stability analysis.

Among the many methods of slope rigid body limitation equilibrium analysis, the Morgenstern–Price method is the only stringent method that does not assume the shape of the slip surface, static equilibrium requirement, and selection method without the assumption of numerous unknown values. Simultaneously, this method can be regressed to a simplified calculation method of most stability analyses. Moreover, the safety factors calculated using simple methods, such as a simplified Bishop method that ignores the inter-slice shear strength, are sometimes large. The safety factors calculated using stringent methods, such as the Morgenstern–Price method (which considers the inter-slice shear strength and the normal stress), are smaller than those obtained by the above methods, and the calculation result is more accurate. Therefore, the Morgenstern–Price method is used to calculate the slope stability in the SLOPE/W module.

3.2 Model building and parameter selection

To ensure the simulation results are maximally in accordance with the reality, the longitudinal section of the slope, which is shown in Fig. 2, is introduced in the SEEP/W module, and the slope calculation model, as displayed in Fig. 3, is established. The slope calculation model has 2218 nodes and 2097 units. First, the seepage field of the slope under rainfall condition is calculated in the SEEP/W module, and subsequently, the calculation results are introduced into the SLOP/W and SIGMA/W modules, respectively. The safety factor, displacement field, and plastic zone of the slope are recalculated under the rainfall conditions.

Based on the results of the drilling exploration and laboratory tests, the overburden on the exit slope of the Chenjiapo tunnel is mainly the silty clay of the landslide accumulation layer and the gravel soil of the residual slope layer of the Quaternary System Holocene Series. Moreover, the underlying strata are mainly the Silurian System Middle Series Shamao Formation siltstone. Based on the indoor tests for the soil and rock samples from a drilling hole (such as moisture content, permeation, and triaxial compression tests), the physical and mechanical parameters of each strata of the 2–2′ section slope are obtained.

From the site survey results, the slope surface is defined as the rainfall boundary condition in the SEEP/W module, the left and right sides of the slope are free permeable boundaries, and the bottom of the slope is an impervious boundary. The slope groundwater level is located at the interface of the rock and the soil. The interface between the rock and the soil is defined as the slip surface in the SLOPE/W module. Horizontal and vertical constraints are applied at the bottom of the slope, and only horizontal constraints are applied on both sides of the slope in the SIGMA/W module.

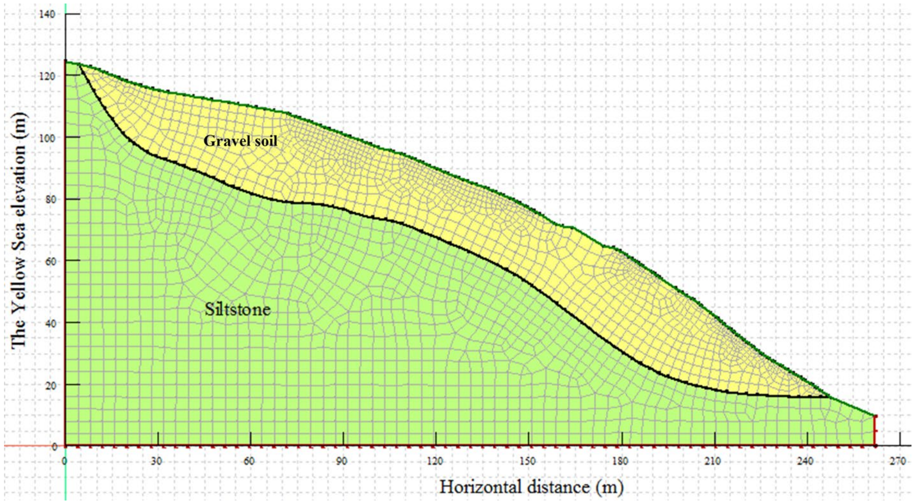

Fig. 3 Calculation model of 2–2′ profile

4 Calculation conditions

Based on the rainfall data provided by the Hydrology and Water Resources Survey Bureau of Enshi Autonomous City of Hubei Province, the monthly average rainfall statistical graphs of the Xuanen County in 2015–2018 are drawn. Figure 4 shows that the total rainfall in the Xuanen County in 2015–2018 is mostly concentrated from May to September, the total monthly rainfall is 200–250 mm, and the maximum rainfall is 388 mm in June 2016. Typical rainfall in the other months is less and approximately 100 mm. The Xuanen County has a subtropical monsoon humid climate, having the characteristics of less cold winter, no summer heat, wet throughout the year, and abundant rainfall. From the statistics of the daily rainfall in the Xuanen County from June 2015 to December 2018, it can also be seen that it is raining most days of every month in the Xuanen County. Specifically, there is mainly light rain, which remains up to 28 days of the month. Heavy or torrential rain in the Xuanen County mainly occurs from April to July, and there are 1–3 days of rainstorms in June and July of every summer, as given in Table 1.

It can be seen from the survey results that the characteristics of frequent rainstorms, continuous rainfall, high-intensity rainfall, and sudden rainfall in spring and summer are the main factors inducing landslides. The average rainfall intensity of rainstorms (50 mm/day $\le$ rainfall intensity $<$ 100 mm/day) in the Xuanen County from June 2015 to April 2019 is approximately 70 mm/day, and the maximum daily rainfall can reach 90 mm/day. Therefore, to study the influence of rainfall on the stability of the exit slope of the Chenjiapo tunnel, combined with the actual rainfall scenario, two rainfall conditions are established: rainstorms with different rainfall types and rainstorms with different rainfall intensities. The parameters of the two rainstorm conditions are listed in Table 2. Under these two rainfall conditions, the effects of different rainfall types and rainfall intensities on the slope stability are studied. As shown in Fig. 5, the rainfall time for each rainfall type is 3 days and the total rainfall amount is 210 mm.

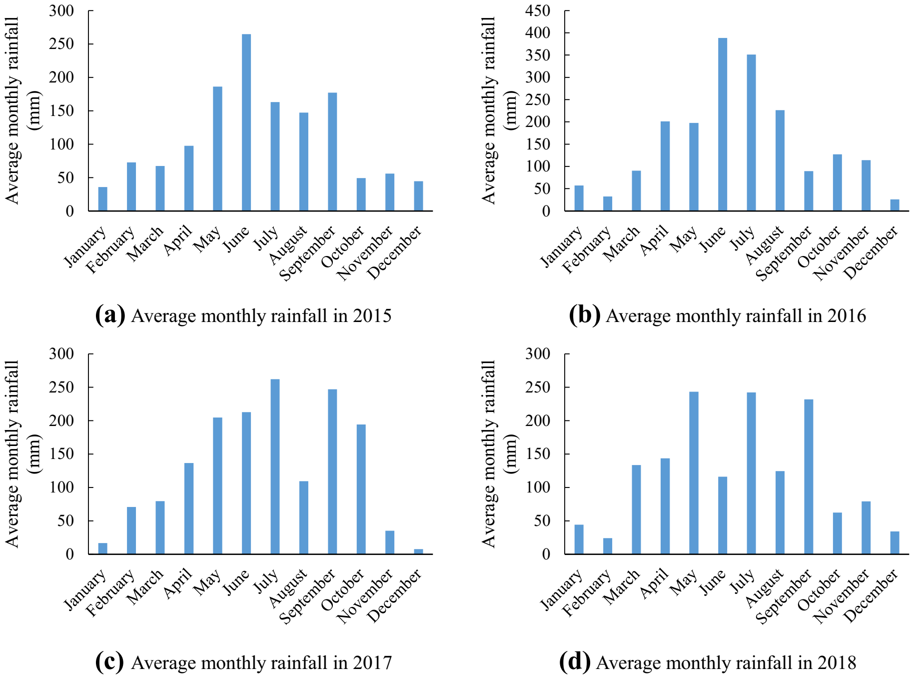

Fig. 4 Average monthly rainfalls in Xuanen County from 2015 to 2018

5 Calculated results and analysis

5.1 Influence of different rainfall types on slope stability

1. Stability analysis of slopes under different rainfall types.

To study the influence of different rainfall types on the slope stability, five rainfall types are established: equal-intensity, stepped, front-peak, medium-peak, and back-peak rainfalls. It can be seen from Fig. 6 that at the same total rainfall, the different rainfall types have a significant influence on the time point of the slope failure. Specifically, under the conditions of equal-intensity and back-peak rainfalls, the safety factors of the slope decrease with the increase in time. Under the equal-intensity rainfall, the safety factor of the slope is relatively stable and reduces from 1.187 to 0.999 at the 36th hour of rainfall, following which the slope begins to lose its stability. Subsequently, the slope safety factor continuously decreases with continuous rainfall and reaches a minimum value of 0.952 at the end of the rainfall, when the slope is further destroyed. Under the condition of back-peak rainfall, the safety factor of the slope reduces from 1.187 to 1.066 on the first day of the rainfall, and although the slope is still in a stable state, the safety margin is not high. Subsequently, the slope safety factor tends to be stable and decreases to a minimum value of 0.955 when the rainfall is concentrated on the third day, following which the slope becomes unstable and is destroyed.

In comparison, under the conditions of stepped, medium-peak, and front-peak rainfalls, the safety factors of the slope first decrease and subsequently increase with the increase in time. However, because of the different rainfall concentration times, the minimum values

Table 1 Physical and mechanical parameters of all strata of slope

Stratum	Saturation bulk density/γ_{sat}(kN/m^3)	Cohesion /c(kPa)	Internal friction angle /φ(°)	Saturated permeability coefficient /k_{sat}(m/day)	Saturated water content /w_{sat}	Poisson ratio /v
Gravel soil	21.8	13.4	26.8	0.663	0.25	0.20
Siltstone	25.6	2030.0	41.3	0.102	0.22	0.17

Table 2 Rainfall conditions and rainfall parameters for Xuanen County

Rainfall conditions	Rainfall intensity	Rainfall days	Rainfall types
Rainstorm with different types	Rainfall amount in 3 days is 210 mm	3 days	Equal-intensity, stepped, front-peak, medium-peak, and back-peak rainfalls
Rainstorm with different intensities	50 mm/day, 70 mm/day, 90 mm/day	3 days	Equal-intensity rainfall

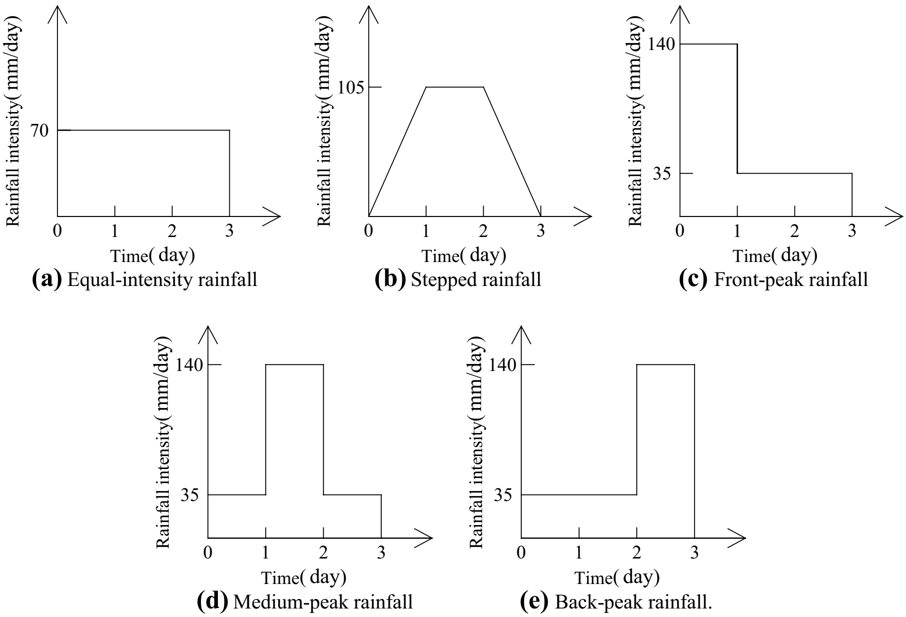

Fig. 5 Different rainfall types (total rainfall in 3 days is 210 mm)

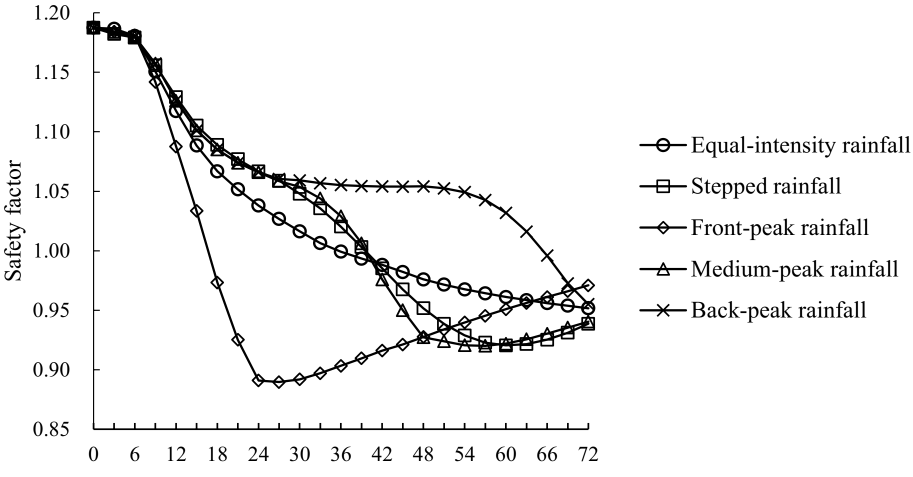

Fig. 6 Change trends of safety factor with increasing of time under different rainfall types (total rainfall in 3 days is 210 mm)

of the three slope safety factors are different. The rainfall distribution characteristics of the stepped rainfall are the same as those of the medium-peak rainfall; therefore, the change tendencies of their slope safety factors are practically same; their safety factors are less than 1 at the 42th hour; and the slope is destroyed. Among them, under the condition of stepped rainfall, the safety factor of the slope reaches a minimum value of 0.921 at the 60th hour. Under the condition of medium-peak rainfall, the safety factor of the slope reaches a minimum value of 0.920 at the 57th hour. The front-peak rainfall is mainly concentrated on the first day of rainfall, and the safety factor of the slope decreases significantly on the first day and decreases to 0.973 at the 18th hour, after which the slope is destroyed. Moreover, among the five rainfall types, the front-peak rainfall slope has the smallest safety factor of 0.890, which occurs at the 27th hour.

2. Analysis of slope displacement field under different rainfall types.

It can be seen from Fig. 7 that the maximum horizontal displacements and safety factors of the slope under the five rainfall types show an opposite trend with the increase in time. Specifically, under the conditions of equal-intensity and back-peak rainfalls, the maximum horizontal displacements of the slope increase with the increase in the rainfall time. Under the conditions of stepped, medium-peak, and front-peak rainfalls, the maximum horizontal displacements of the slope first increase and then decrease with an increase in rainfall time. Because of the different rainfall concentration periods of the five rainfall types, the maximum horizontal displacements occur at different times. Because the equal-intensity and back-peak rainfalls do not decrease with the increase in time, their maximum horizontal displacements are 0.218 and 0.229 m, respectively, at the end of the rainfalls. The maximum horizontal displacement of the stepped rainfall slope is 0.228 m at the 57th hour. The maximum horizontal displacement of the medium-peak rainfall slope is 0.231 m at the 48th hour. The maximum horizontal displacement of the front-peak rainfall slope is 0.233 m at the 24th hour. Subsequently, because the rainfall amounts of the three rainfall types decrease, particularly of the medium-peak and front-peak rainfalls, which decrease abruptly, the rainwater infiltration inside the slope decreases and the horizontal displacement of the slope has a small rebound.

It can be seen from Fig. 8 that the horizontal displacements of the slope under the five rainfall types occur at the bottom of the slope, and the slope presents clear traction failure

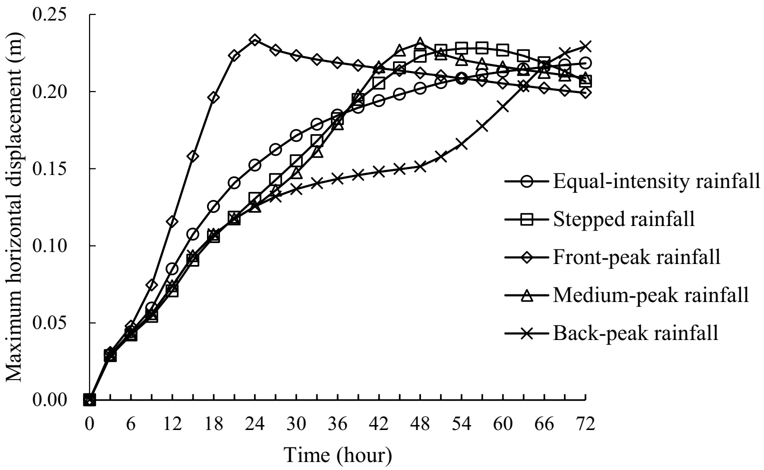

Fig. 7 Change trends of maximum horizontal displacement with increasing time under different rainfall types (total rainfall in 3 days is 210 mm)

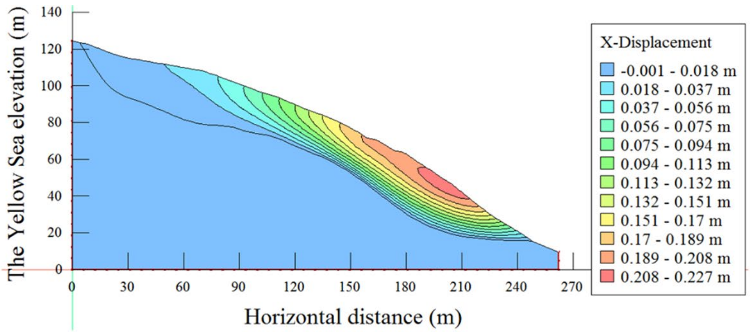

(a) Equal-intensity rainfall (72th hour, maximum horizontal displacement is 0.218 m)

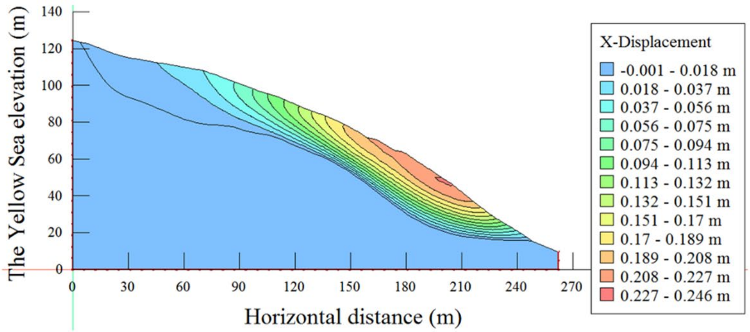

(b) Stepped rainfall (57th hour, maximum horizontal displacement is 0.228 m)

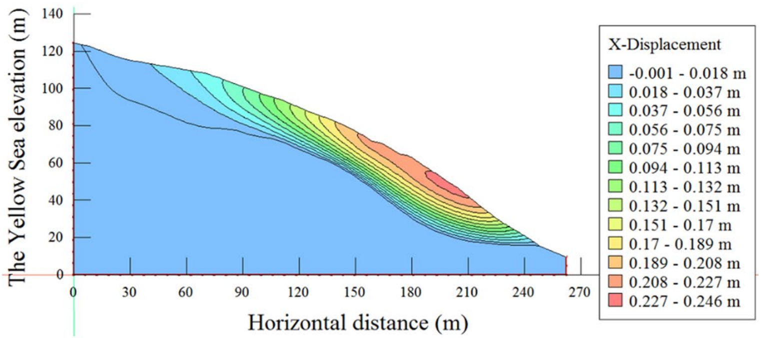

(c) Front-peak rainfall (24th hour, maximum horizontal displacement is 0.233 m)

Fig. 8 Maximum horizontal displacement diagram of the slope under different rainfall types (total rainfall in 3 days is 210 mm)

characteristics. The results show that sliding failure occurs at the bottom of the slope, and the simulation results are consistent with the survey results. In addition, under the condition of front-peak rainfall, the maximum horizontal displacement distribution range of the slope is larger than those of the other four rainfall types. Among all the rainfall types, under the condition of front-peak rainfall, the maximum horizontal displacement is the first

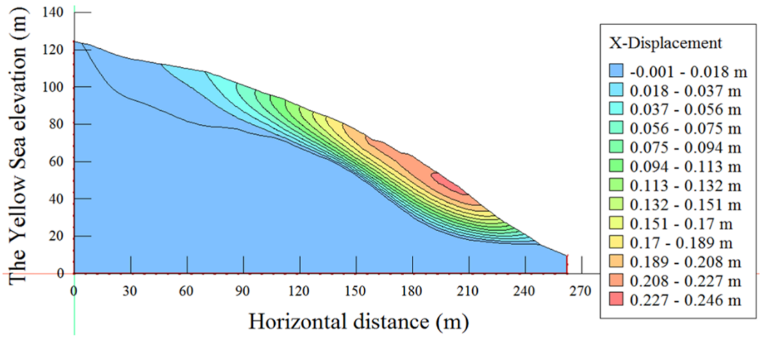

(d) Medium-peak rainfall (48th hour, maximum horizontal displacement is 0.231 m)

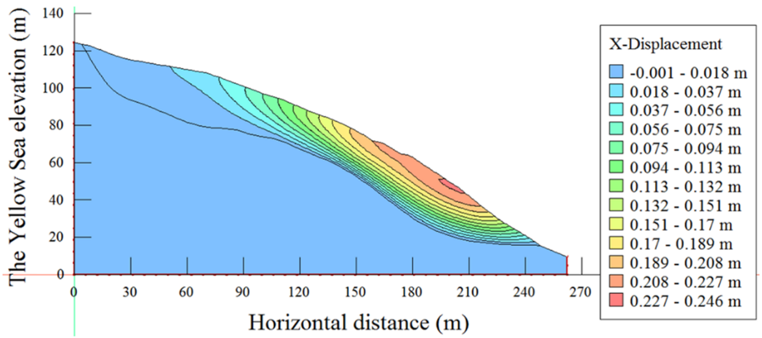

(e) Back-peak rainfall (72th hour, maximum horizontal displacement is 0.229 m)

Fig. 8 (continued)

to reach 0.233 m and is the largest. Therefore, the front-peak rainfall is the most unfavorable for the slope stability under the same total rainfall and rainfall time.

3. Analysis of the change in the plastic zone of slope under different rainfall types.

As shown in Figs. 9, 10, 11, 12, and 13, under the conditions of equal-intensity, stepped, and medium-peak rainfalls, it can be seen that the change trends of the plastic zone of the slope are basically the same during continuous rainfall. The plastic zone distribution of the slope is small on the first day, and the plastic zone is mainly located at the foot of the slope and the slide zone and is relatively less around the slope top and the slope surface. On the second day of the rainfall, the plastic zone of the slope is completely through the upper soil layer, and the slope is unstable and destroyed. Owing to the scarcity of rainfall on the first two days, under the condition of back-peak rainfall, the plastic zone of the slope develops gradually. The plastic zone of the slope is mainly distributed at the foot of the slope and the slip zone on the first day of the rainfall, and the distribution range is relatively small. Compared to the first day, the distribution range of the plastic zone increases slightly, and the slope remains in a stable state on the second day of the rainfall. Under the condition of the back-peak rainfall, the plastic zone of the slope develops rapidly after the third day of the rainfall, the plastic zone is completely through the upper soil layer at the end of the rainfall,

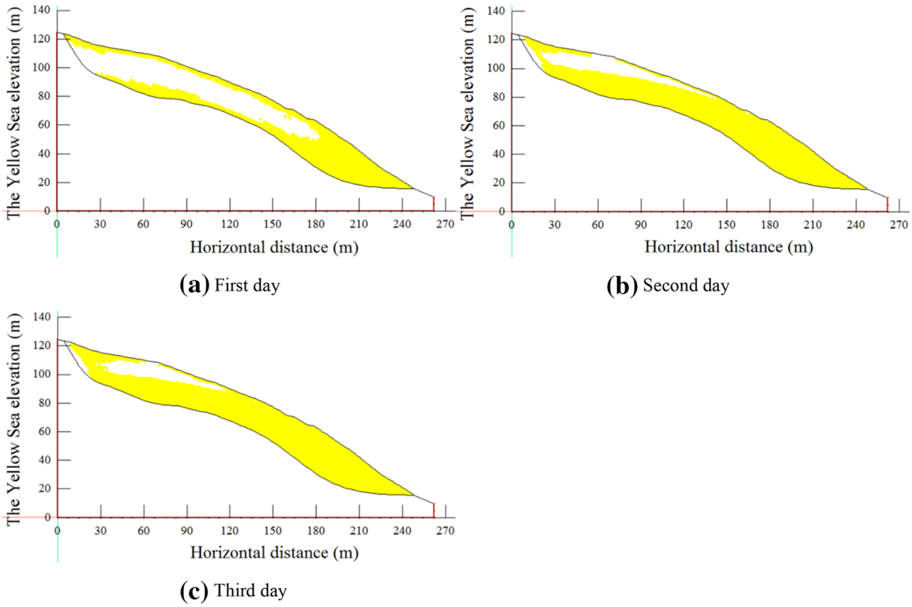

Fig. 9 Variation process of plastic zone of slope under equal-intensity rainfall (total rainfall in 3 days is 210 mm)

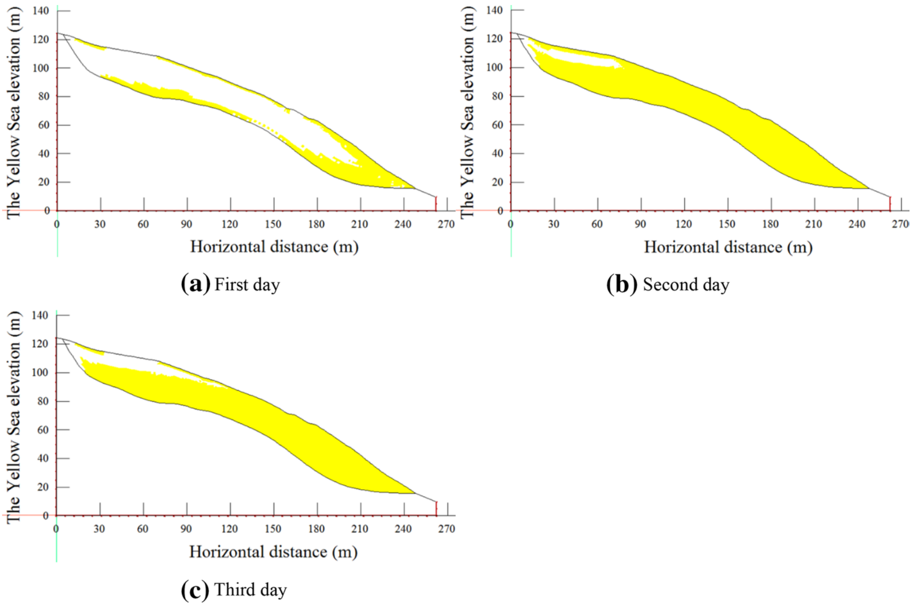

Fig. 10 Variation process of plastic zone of slope under stepped rainfall (total rainfall in 3 days is 210 mm)

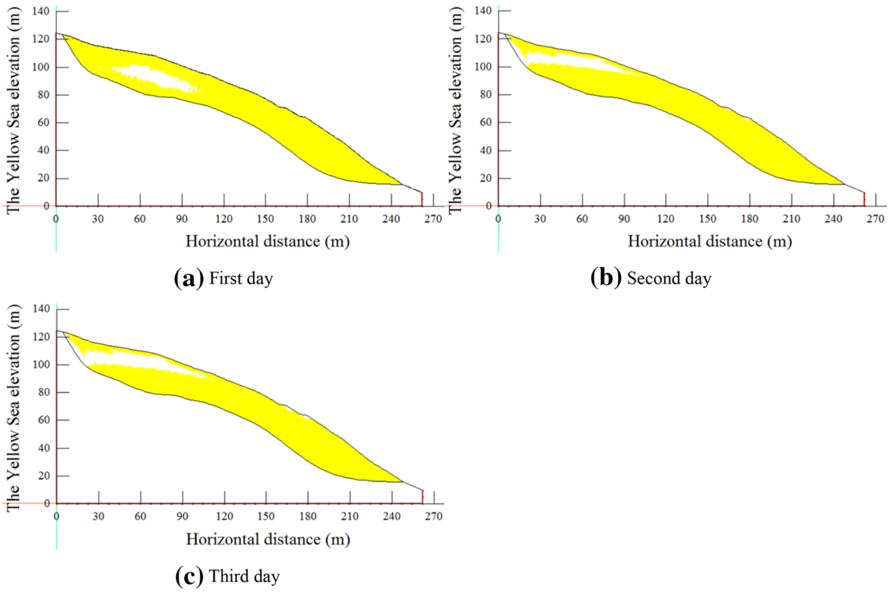

Fig. 11 Variation process of plastic zone of slope under front-peak rainfall (total rainfall in 3 days is 210 mm)

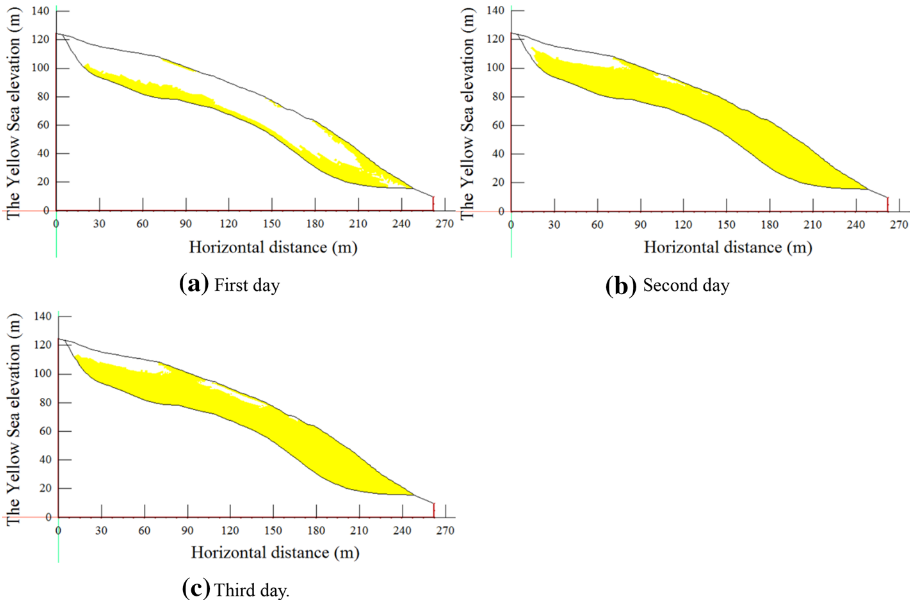

Fig. 12 Variation process of plastic zone of slope under medium-peak rainfall (total rainfall in 3 days is 210 mm)

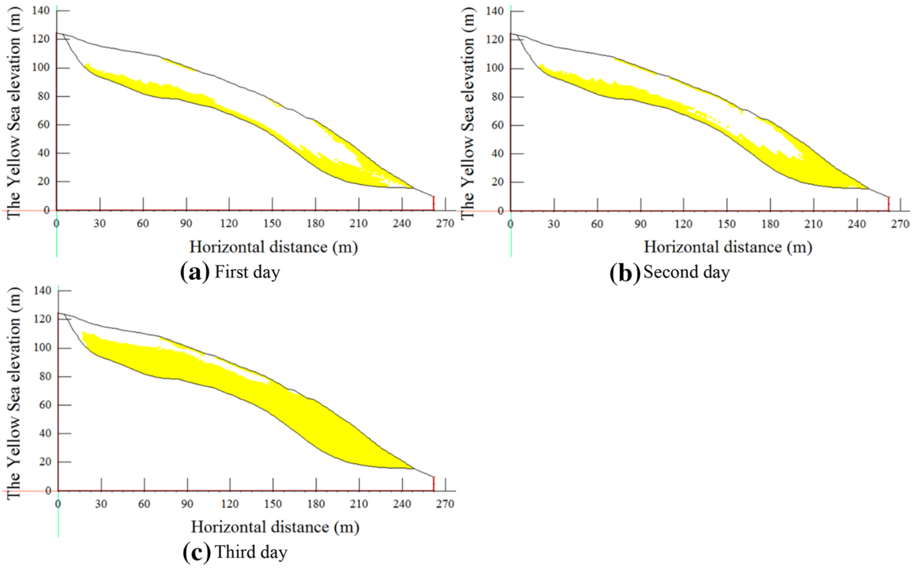

Fig. 13 Variation process of plastic zone of slope under back-peak rainfall (total rainfall in 3 days is 210 mm)

and the stability of the slope decreases rapidly until failure. The front-peak rainfall is mainly concentrated on the first day; therefore, the plastic zone develops more rapidly than under the other rainfall types. The plastic zone of the slope is completely through the upper soil layer on the first day of the rainfall, the distribution range of the plastic zone is larger than those under the other rainfall types, and the slope is destroyed at the end of the first day of the rainfall.

Comparing the changes in the safety factor, displacement, and plastic zone of the slope under the conditions of the five rainfall types, it can be seen that their influence degrees on the slope stability are different for the same total rainfall. First, the influence of the stepped rainfall on the slope stability is basically the same as that of the medium-peak rainfall. The influence of the stepped and medium-peak rainfalls on the slope stability shows consistent trends in three aspects: slope safety factor, horizontal displacement, and plastic zone development. Subsequently, the equal-intensity and back-peak rainfalls show the same trends in the change in the slope stability; however, the time points of the slope failure are different. Because the back-peak rainfall is mainly concentrated on the third day, the slope stability with the rainfall of the previous two days is relatively better. With the abrupt increase in the rainfall on the third day, a large amount of rainwater infiltration occurs, which causes an increase in the slope gravel soil weight, a decrease in the shear strength, instability, and failure of the slope. Finally, among all the rainfall types, the front-peak rainfall has the greatest adverse effect on the slope stability. Because the front-peak rainfall is mainly concentrated on the first day, the stability of the slope decreases rapidly in the initial stage of the rainfall. A large amount of rain infiltration directly occurs, which leads to a rapid saturation of the slope soil, and the slope is destroyed at the end of the first day of the rainfall.

5.2 Influence of rainfall intensity on slope stability

1. Analysis of slope stability under different rainfall intensities.

Three rainfall intensities of 50 mm/day, 70 mm/day, and 90 mm/day are selected to study their influence on the slope stability. The calculation time is 15 days, the rainfall duration is the first 3 days of the 15 days, and the rainfall type is equal-intensity rainfall. It can be seen from Fig. 14 that the slope safety factors show the same trends for the calculation time under the three rainfall intensities. On the first three days of the rainfall duration, under the three rainfall intensities, the slope safety factors decrease with the increase in the time. When the rainfall intensity is 50 mm/day, the slope safety factor reaches a minimum value of 1.023 at the end of the rainfall. Although the slope is not destroyed, the safety margin is not high. When the rainfall intensity is 70 mm/day, the slope begins to lose its stability at the 36th hour of the rainfall. With the continuation of the rainfall, the slope stability continues to decrease, and the slope safety factor reaches a minimum value of 0.952 at the end of the rainfall. When the rainfall intensity is 90 mm/day, it takes a shorter time for the slope to be destroyed than under the 50 mm/day and 70 mm/day rainfall intensities. Moreover, the slope is destroyed at the 27th hour. The slope stability is worse at the end of the rainfall, and the safety factor of the slope under the 90 mm/day rainfall intensity has the minimum value of 0.887 among those of the three rainfall intensities.

After the end of the rainfall, the slope safety factors under the three rainfall intensities initially increase rapidly and subsequently gradually stabilize. After the rainfall stops, with the continuous infiltration and discharge of the rain inside the slope, the saturation line of the slope moves downward, and the upper soil of the slope is restored from the saturation state to an unsaturated state. Moreover, the shear strength of the soil is gradually improved and the slope stability is also gradually increasing. It can be seen from Fig. 14 that the safety factors of the slope under the three rainfall intensities are basically the same at the

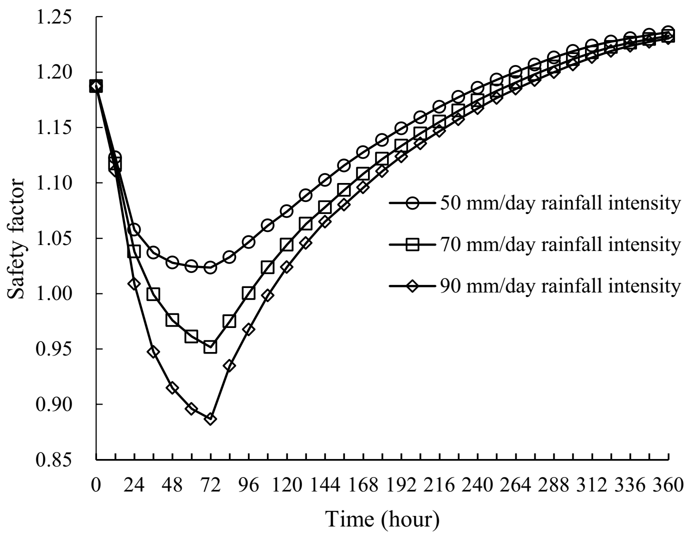

Fig. 14 Change trends of safety factor with increasing of time under different rainfall intensities (equal-intensity rainfall for 3 days)

end of the computation. This shows that a high rainfall intensity during the rainfall process is associated with a short time required for the failure of the slope, and the slope stability is also the worst at the end of the rainfall. However, within 12 days after the end of the rainfall, the slope stability under the three rainfall intensities can be restored to the same stable state.

2. Analysis of slope displacement field with increase in time under rainfall intensity of 70 mm/day.

As shown in Fig. 15, it can be seen that the trend of the maximum horizontal displacement curve of the slope under the rainfall intensity of 70 mm/day is opposite to that of the safety factor curve of the slope with the increase in the time. During the rainfall, because of rain infiltration, the upper soil layer of the slope changes from an unsaturated to a saturated state, the shear strength of the soil decreases, a horizontal displacement of the slope occurs, and the stability of the slope decreases. At the end of the third day of the rainfall, the horizontal displacement of the slope reaches 0.218 m, and the slope is destroyed. After the end of the rainfall, with the infiltration and discharge of the rain inside the slope, the stability of the slope is restored, and the horizontal displacement of the slope gradually rebounds. At the end of the computation, the horizontal displacement of the slope is restored to 0.067 m, and the slope is in a stable state. As can be seen in Figs. 8a and 16, the maximum horizontal displacement of the slope decreases gradually after the end of the rainfall and it also occurs at the foot of the slope. With the failure of the slope foot, the upper part of the slope loses its support and slips downward under the action of self-weight, and the entire slope is destroyed, and the slope presents clear traction failure characteristics. However, the maximum horizontal displacement of the slope is only 0.067 m at the end of the computation, and the distribution area of the slope failure is reduced, which has little influence on the stability of the slope and shows that the slope has to be restored to a stable state.

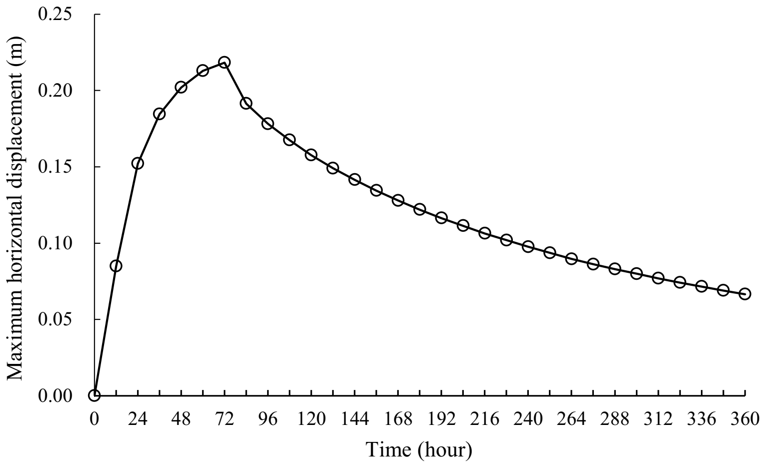

Fig. 15 Change trends of maximum horizontal displacement with increasing time under 70 mm/day rainfall intensity (equal-intensity rainfall for 3 days)

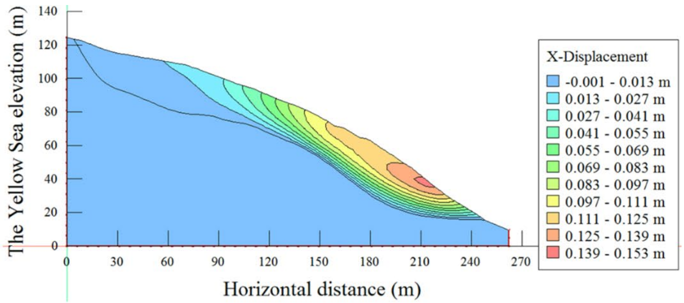

(a) Sixth day, maximum horizontal displacement is 0.142 m

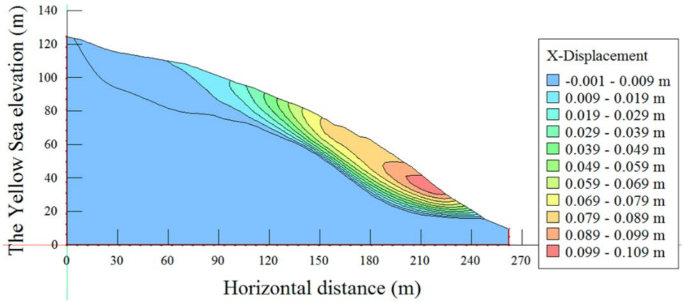

(b) Ninth day, maximum horizontal displacement is 0.106 m

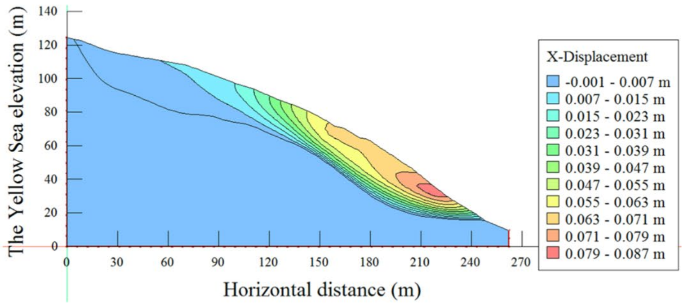

(c) Twelfth day, maximum horizontal displacement is 0.083 m

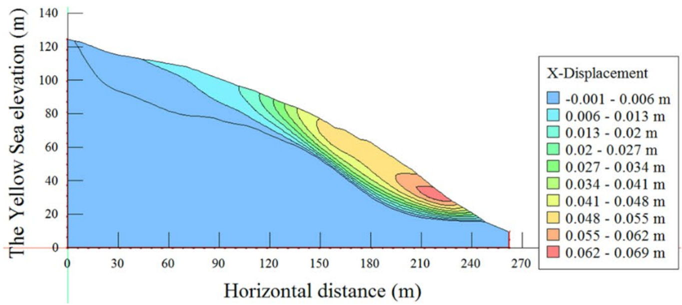

(d) Fifteenth day, maximum horizontal displacement is 0.067 m

Fig. 16 Variation in displacement of slope under 70 mm/day rainfall intensity (equal-intensity rainfall for 3 days)

3. Analysis of change in plastic zone of slope under rainfall intensity of 70 mm/day.

From Figs. 9 and 17, on the third day after the end of the rainfall, with the increase in the shear strength of the soil in the upper layer of the slope, the distribution range of the plastic zone of the slope is significantly reduced than that at the end of the rainfall. The plastic zone of the slope is mainly distributed at the foot of the slope and scattered on the surface of the slope and the slip zone. It can also be seen from Figs. 17b–d that with the increase in time, the distribution range of the plastic zone of the slope continues to decrease after the end of rainfall. Moreover, the plastic zone is only separately distributed at the foot surface and the sliding zone of the slope, and the slope gradually returns to stability. In addition, during the rainfall, the plastic zone first distributes at the foot of the slope and subsequently gradually through the entire slope, resulting in the failure of the slope. The distribution of the plastic area of the slope begins to decrease after the end of the rainfall, and compared with other parts of the slope, the foot of the slope is still the most widely distributed area of the plastic zone. Therefore, the result shows that the slope has clear traction failure characteristics from either the slope displacement field or the plastic area distribution range. Rainfall causes rainwater to infiltrate and collect at the bottom of the slope, and the foot of the slope is first destroyed. After the upper part of the slope loses its support, the slope undergoes complete failure.

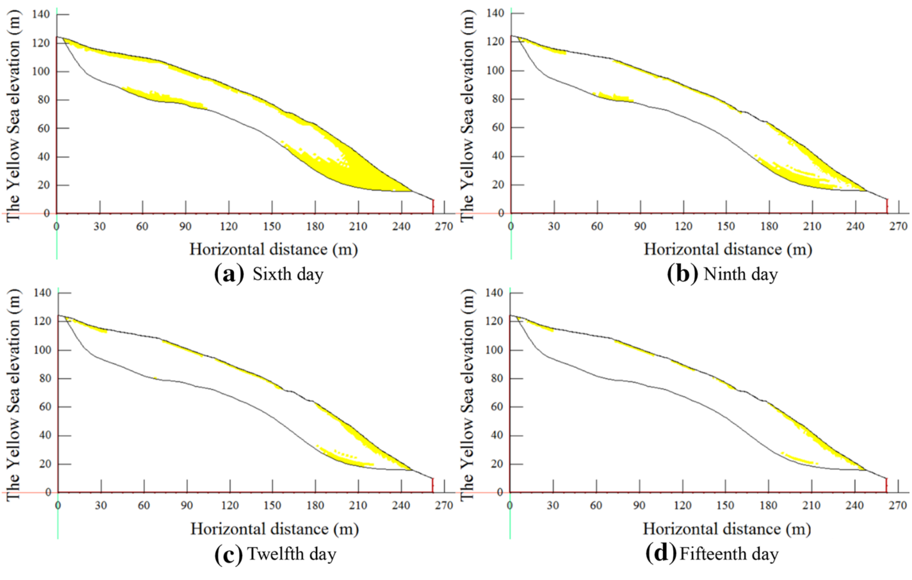

Fig. 17 Plastic zone change of slope after end of rainfall under 70 mm/day intensity (equal-intensity rainfall for 3 days)

6 Conclusions

(1) The exit slope of the Chenjiapo tunnel is located in Xuanen County, Hubei Province. The geological structure is a hidden fault structure with a natural slope of 22–26° and a downward slope. The overburden on the slope is mainly gravel soil, the other part of the overburden is silty clay, and the underlying bedrock is siltstone. The yearly rainfall of Xuen County is 1361–1902 mm, and its maximum daily rainfall value is 90 mm. Continuous rainfall, high-intensity rainfall, and sudden rainfall in spring and summer are the main factors inducing landslides. The slope is located directly above the exit of the Chenjiapo tunnel. During the excavation of the tunnel, the left side of the front edge of the slope slipped downward, and a sliding landslide and an unstable slope are formed under the action of rainfall and excavation. The width, longitudinal length, and volume of the sliding landslide are approximately 120 m, 70 m, and approximately 6.27×10^4 m^3, respectively, and it is a large-type landslide. The landslide has threatened the safe construction of the tunnel, and the tunnel is in a state of shutdown. The width, longitudinal length, and volume of the unstable slope are approximately 200 m, 300 m, and 8.69×10^5 m^3, respectively. The unstable slope not only threatens the safe construction of the tunnel but also directly risks the operation safety of the expressway at a later stage.

(2) The safety factor of the slope decreases with the increase in the rainfall time under the conditions of equal-intensity, stepped, medium-peak, and back-peak rainfalls. Under the conditions of stepped and medium-peak rainfalls, the safety factors of a slope rise slightly on the third day of the rainfall. The slopes of the four rainfall types begin to be destroyed in the middle and late stages of the rainfall, and the plastic zone begins to be completely through the slope. Compared to the slope safety factors of the four rainfall types, that under the front-peak rainfall first decreases and subsequently increases with the increase in time. Moreover, the failure occurs in the 18th hour of the rainfall which is the earliest time of slope failure, and the plastic zone is completely through the upper soil layer at the end of the first day of rainfall. Under the condition of front-peak rainfall, the maximum horizontal displacement of the slope is also the maximum value among those of the five rainfall types, and it can reach 0.233 m. Therefore, under the same rainfall duration and total rainfall, the front-peak rainfall is the most harmful to the slope.

(3) Under the condition of three days of equal-intensity rainfall, the minimum safety factor of the slope under a 50 mm/day rainfall intensity is 1.023, and no failure occurs. The minimum safety factor of the slope under the 70 mm/day rainfall intensity is 0.952, which begins to destroy at the 36th hour of the rainfall. The minimum safety factor of the slope under the 90 mm/day rainfall intensity is 0.887, which begins to destroy at the 27th hour of the rainfall. This shows that a high rainfall intensity is related to the short time required for slope failure. Moreover, the worse the slope stability is at the end of the rainfall, the more unfavorable the slope stability becomes. The safety factor of the slope immediately rebounds after the rainfall, the horizontal displacement gradually rebounds, the distribution range of the plastic zone begins to decrease, and the slope has returned to a stable state after 12 days of the rainfall end.

(4) Based on the results of the numerical simulation and comprehensive analysis, the slope is unstable and damaged under rainstorm conditions. Therefore, it is suggested that the exit slope of the Chenjiapo tunnel should be strengthened by mainly building anti-slide piles to retain with closing slope cracks and draining as the subsidiary on the slope

and other methods. Rows of anti-slide piles are arranged in the upper part of the tunnel exit and the front part of the sliding landslide body. Simultaneously, drainage holes are added at the front edge of the sliding landslide body and a drainage seepage ditch is arranged along the back edge of the sliding landslide body to drain the surface water. Clay or mortar is used to seal the cracks on the slope in time to prevent rainwater from infiltrating the slope and causing sliding again.

Funding Project (51509211) supported by National Natural Science Foundation of China; Project (2016M602863) supported by China Postdoctoral Science Foundation; Project (2018031) supported by Excellent Science and Technology Activities Foundation for Returned Overseas Teachers of Shaanxi Province; Project (2015SF260) supported by Social Development Foundation of Shaanxi Province; Project (2017BSHYDZZ50) supported by Postdoctoral Science Foundation of Shaanxi Province; Project (2016GY-01) supported by Yangling District Foundation; Project (2452020169) supported by the Fundamental Research Funds for the Central Universities; Project (A213021602) supported by International Cooperation Foundation of Northwest A&F University; Project (A213021803) supported by Foreign Cultural and Educational Experts Foundation of Northwest A&F University.

References

Bednarczyk Z (2018) Identification of flysch landslide triggers using conventional and 'nearly real-time' monitoring methods - An example from the Carpathian Mountains, Poland[J]. Eng Geol 244:41–56
Dou H-Q, Wang H (2017) Probabilistic analysis of spatial variability of saturated hydraulic conductivity on infinite slope based on the non-stationary random field [J]. China Civil Eng J 50(8):105–113
Gao L-T, Yan E-C, Liu Ke (2014) Study on multi-field characteristics of accumulated landslide considering rainfall conditions[J]. J Eng Geol 22(2):263–271
Garcia-Delgado H, Machuca S, Medina E (2019) Dynamic and geomorphic characterizations of the Mocoa debris flow (March 31, 2017, Putumayo Department, southern Colombia)[J]. Landslides 16(3):597–609
Hou T-S, Wang X-G, Pamukcu S (2016) Geological characteristics and stability evaluation of Wanjia middle school slope in Wenchuan Earthquake Area[J]. Geotech Geol Eng 34(1):237–249
Hou T-S, Xu G-l, Shen Y-J, Wu Z-Z, Zhang N-N, Wang R (2013) Formation mechanism and stability analysis of the Houba expansive soil landslide[J]. Eng Geol 161:34–43
Huang J-H, Chen C-H, Qin W-T (2017) Reliability analysis of two-dimensional slope stability under rainfall conditions[J]. J Fuzhou Univ (Nat Sci Ed) 45(2):501–507
Ze-feng J, Da-yong Z, Yin-bin S, Bao-cun W (2015a) Critical slip field of slope under the condition of transient unsaturated seepage[J]. Rock Soil Mech 36(6):1815–1823
Jiang Z-M, Wu Z-C, Feng S-R, Zhong H-y, Wang J-Y, Wang G-Y (2015b) Limit equilibrium analysis method of slope stability considering transient saturation zone[J]. J Hydraul Eng 46(7):773–782
Kong Y-F, Song E-X, Yang J, Zhang L-Y, Shi H-G, Liu J (2013) Rainfall′s effect on the stability of unsaturated slopes[J]. J Civil, Archit Environ Eng 35(6):16–21
Arishma R, Brook MS, Cronin SJ (2019) Engineering geomorphological investigation of the Kasavu landslide, Viti Levu, Fiji[J]. Landslides 16(7):1341–1351
Rong G, Wang S-J, Wang E-Z, Wang J-X (2008) Stability analysis of yuanmo highway slope under intensive rainfall[J]. Chin J Rock Mechan Eng 27(4):704–711
Santo A, Di Crescenzo G, Forte G, Papa R, Pirone M, Urciuoli G (2018) Flow-type landslides in pyroclastic soils on flysch bedrock in southern Italy: the Bosco de' Preti case study[J]. Landslides 15(1):63–82
Shi Z-M, Shen D-H, Peng M, Zhang L-l, Zhang F-W, Zheng X-Z (2016) Slope stability analysis considering rainfall infiltration of multi-layer unsaturated soil[J]. J Hydraul Eng 47(8):977–985
Tang D, Li D-Q, Zhou C-B, Fang G-G (2013) Slope stability analysis considering antecedent rainfall process[J]. Rock Soil Mech 34(11):3239–3248

Wang B, Vardon PJ, Hicks MA (2018) Rainfall-induced slope collapse with coupled material point method[J]. Eng Geol 239:1–12
Xu H, Zhu Y-W, Cai Y-q, Zhu F-M (2005) Stability analysis of unsaturated soil slopes under rainfall infiltration[J]. Rock Soil Mech 26(12):1957–1962
Yang KH, Thuo JN, Chen JW, Liu CN (2019) Failure investigation of a geosynthetic-reinforced soil slope subjected to rainfall[J]. Geosynth Int 26(1):42–65
Yang KH, Uzuoka R, Lin GL, Nakai Y (2017) Coupled hydro-mechanical analysis of two unstable unsaturated slopes subject to rainfall infiltration[J]. Eng Geol 216:13–30
Ye S-H, Shi T-L (2018) Stability analysis of multi-stage high slope with loess under rainfall infiltration[J]. J Eng Geol 26(6):1648–1656
Yu Y-Z, Lin H-Z, Li R-J, Li G-X (2008) Stability analysis of unsaturated soil slope under transient seepage flow state[J]. Rock Soil Mech 29(11):2892–2898
Zeng L, Li G-y, Shi Z-N, Qiu X, Bian H-B, Li D-k (2018) Effect of antecedent rainfall on characteristics and stability of unsaturated overburden slope[J]. J Cent South Univ (Sci Technol) 49(1):3239–3248
Zhang L-y, Chen T-L, Zhang D-l (2019) Progressive failure of expansive soil slopes under rainfall[J]. Chin J Geotech Eng 41(1):70–77
Zhan W-T, Xiao J, Chen G-y, Chang J (2018) Numerical simulation of seepage and stability analysis of expansive soil slope[J]. Ind Constr 48(9):133–139
Zhao L-H, Li D-J, Tan H-H, Cheng X, Zuo S (2019) Characteristics of failure area and failure mechanism of a bedding rockslide in Libo County, Guizhou, China[J]. Landslides 16(7):1367–1374

Authors and Affiliations

Xiang Duan[1] · Tian-shun Hou[1] · Xiao-dong Jiang[1]

✉ Tian-shun Hou
houtianshunyx@sina.com
http://blog.sciencenet.cn/u/houtianshunyx

1 College of Water Resources and Architectural Engineering, Northwest A&F University, No. 23 Weihui Road, Yangling 712100, Shaanxi, China